Extended Hubbard model: Charge ordering and Wigner-Mott transition

A. Amaricci, A. Camjayi, K. Haule, and G. Kotliar
Department of Physics and Astronomy, Rutgers University, Piscataway, New Jersey 08854, USA

D. Tanasković
Scientific Computing Laboratory, Institute of Physics Belgrade, Pregrevica 118, 11080 Belgrade, Serbia

V. Dobrosavljević
Department of Physics and National High Magnetic Field Laboratory, Florida State University, Tallahassee, Florida 32306, USA

(Received 19 May 2010; revised manuscript received 23 July 2010; published 1 October 2010)

Strong correlations effects, which are often associated to the approach to a Mott insulating state, in some cases may be observed even far from half filling. This typically happens whenever the intersite Coulomb repulsion induces a tendency toward charge ordering, an effect that confines the electrons, and in turn favors local moment formation, i.e., Mott localization. A distinct intermediate regime then emerges as a precursor of such a Wigner-Mott transition, which is characterized by both charge and spin correlations, displaying large mass enhancements and strong renormalizations of other Fermi-liquid parameters. Here we present a careful study of a quarter-filled extended Hubbard model—a simple example where such physics can be studied in detail, and discuss its relevance for the understanding of the phenomenology of low-density two-dimensional electron gases.

DOI: 10.1103/PhysRevB.82.155102 PACS number(s): 71.27.+a, 71.30.+h

I. INTRODUCTION

Early theoretical and experimental investigations of two-dimensional electron gases (2DEGs) largely focused on disorder effects that dominate the so-called "diffusive" regime $k_BT \ll \hbar/\tau$, τ being the impurity scattering rate. In this situation, which is best realized in relatively low-mobility materials, the interaction effects are expected to be weak and coherent multiple-scattering processes dominate—ultimately leading to the formation of bound electronic states through Anderson localization. This impurity effect was first predicted in the famed scaling theory of localization,[1] for noninteracting and weakly disordered 2DEG systems, and was quickly extended to include the weak interaction corrections.[2] The predicted logarithmic rise of the resistivity at low temperature was soon confirmed by experiments on thin metallic films and two-dimensional semiconducting surfaces.[3,4] All this intensive activity around the 2DEG contributed to the emergence of a widely held opinion that, in these systems, even a minute amount of (impurity) disorder will localize all the electronic states at $T=0$. If this were true, then there should not exists a sharp metal-insualtor transition (MIT) in any two-dimensional system; the density and/or temperature dependence of transport should simply reveal a gradual crossover from weak to strong localization.

Given this conventional lore focusing on disorder effects, the 1994 pioneering experiment of Kravchenko *et al.*[5] provided quite a surprise. It reported low-temperature transport behavior in ultraclean 2D silicon samples which, around this time, became available due to technological advances in fabricating semiconductor devices. Kravchenko's work presented first evidence for dramatic changes in the temperature dependence of the resistivity in a narrow density range, suggesting the possibility of a MIT in the 2DEG. This result—quite surprisingly—passed almost unnoticed for several years, until confirmed by independent transport and magnetic response measurements on clean Si-metal-oxide-semiconductor field-effect transistor,[6] as well as on other semiconductor heterostructures (e.g., GaAs/AlGaAs).[7] These results have attracted a great deal of attention to this field, triggering a surprising variety of proposed theoretical scenarios,[8] many of which were quickly ruled out on experimental grounds.[9]

A. Strong correlations revealed

The next 10 years produced significant new information from complementary studies by several groups, which reported singular enhancement of the effective mass,[9] $m^* \sim (n-n_c)^{-1}$, and emphasized the central role played by spin physics in the low-density 2DEG systems. In particular, experimental measurements of the electronic spin susceptibility in the proximity of the MIT shown a Curie-Weiss behavior $\chi/n \simeq g\mu_B^2/T$, suggesting almost total conversion of the electrons into local magnetic moments below the critical density.[10–12] While the initial attention concentrated on the role of disorder,[13] more recent experiments[9] made it increasingly clear that many key experimental features seem to persist even in the cleanest samples, thus pointing to effects intrinsic to the low-density 2DEG. All these experimental results have contributed to validate the emerging idea[14,15] that *strong interactions are the primary driving force* behind the instability of the Fermi liquid phase in favor of an insulating state in the low-density 2DEG.

In very recent work,[14,15] radically new ideas have been put forward to explain the observed behavior, and to reconcile the early viewpoint of Wigner with the possibility of Mott physics in the low-density regime. According to this *Wigner-Mott scenario*[14,15] the rich phenomenology of the 2DEG is ultimately determined by the competition between the *long-range* Coulomb interaction and the kinetic energy.

As first noted by Wigner,[16,17] both the Coulomb interaction E_C and the kinetic (Fermi) energy E_F decrease with decreasing density n but their ratio $r_s = E_C/E_F$, i.e., the Wigner-Seitz radius, increases. Thus, the Coulomb repulsion is expected to dominate at very low densities ($r_s \gg 1$) and low enough temperatures, leading to the formation of a charge-ordered state—a *Wigner crystal.* In this regime each electron forms a bound state within a potential well formed by the repulsion from other electrons, and must overcome an activation gap to escape. In the opposite regime ($r_s \ll 1$), the quantum fluctuations lead to the eventual melting of the Wigner lattice, and the consequent formation of a homogeneous Fermi-liquid state. In between these two limits, the system is expected to undergo a series of nontrivial transformations, making the description of the phase diagram of the 2DEG one of the most challenging tasks of modern condensed-matter physics.

B. Driving force: Interactions or disorder?

This Wigner-Mott scenario should be contrasted with the alternative physical picture as first proposed in the early theoretical works of Refs. 18 and 19. Here disorder is envisioned as the primary driving force for electron localization, and the insulator consists of Anderson-localized electrons bound to impurities. In this scenario, the primary role of the interactions is to stabilize the metallic state at higher densities, a possible mechanism that has been explored in relatively recent theoretical work.[13] The key theoretical challenge, therefore, is to carefully identify the precise consequences of each of these physical pictures, and assess their respective relevance in light of experiments.

In this work we focus on the understanding of the role of the electronic correlation in the Wigner transition, thus we shall deliberately *disregard* all disorder effects, and focus on investigating the predictions of the Wigner-Mott picture, which we believe can account for most qualitative aspects of the puzzling experimental features.

To understand how the Mott physics, usually ascribed to half-filled narrow bands, emerges out of the low-density 2D systems, one should consider the following argument. A barely melted Wigner crystal is dominated by the local spin correlations while the short-range Coulomb repulsion largely precludes double occupations. Therefore, it becomes reasonable to view a metal in the vicinity of Wigner crystallization as a system on the brink of Mott localization. Physically, in the $r_s \gg 1$ regime, the Coulomb interaction proves so strong that it keeps all the electrons at bay, even after the crystal has melted. The volume fraction available for each electron is thus significantly reduced, giving rise to the "confinement" of each electron. This situation is *locally* close to half filling and the Mott regime, hence providing an explanation for the (observed) similarities of a dilute 2D electrons gas with conventional Mott materials characterized by narrow half-filled bands.

While of plausible significance for diluted 2DEG, the phenomenon of Wigner-Mott localization applies to many more systems. In fact, based on the general arguments of Wigner, one may expect that it will emerge for any partially filled band, where intersite (long-range) Coulomb interactions are able to induce charge ordering. These effects have generally been little explored, and were so far mostly studied in (quasi-) one-dimensional systems.[20,21] However, recent detailed experimental studies on charge-ordering phenomena in layered organic molecular crystals,[22] and on the cobalt oxide Na_xCoO_2,[23] have triggered several theoretical investigations of extended Hubbard models (EHMs) which includes both on-site and nearest-neighbor interaction.[24–26] Some aspects of the resulting behavior may be influenced by material-specific details, such as the form of the lattice. In compounds with triangular lattice structure, for example, geometrical frustration leads to the competition of several ground states.[27] Although still relatively few, all these examples indicate that Wigner-Mott localization is clearly a very general phenomenon, which is yet to be explored in detail. Its experimental realizations are often found in two-dimensional systems, where device geometries (e.g., gating the 2DEG) allows easy control of carrier density, which facilitates accessing the low-density transition region. Still, as a matter of principle, this phenomenon is not restricted to $d=2$, and thus should be found in all dimensions. In addition, the charge-density wave (CDW) ordering underpinning can emerge not only for both long-range intersite (Coulomb) interactions but also for sufficiently strong short-range (e.g., nearest-neighbor) repulsion.[28]

To gain insight into its generic features, in this paper we restrict our attention to the *simplest model* that illustrates its fundamental mechanism: Mott localization as driven by charge ordering. This is accomplished by carefully examining the quarter-filled EHM,[29,30] which we solve using single-site dynamical mean-field theory[31] (DMFT) methods and a combination of several quantum impurity solvers. The EHM has already been studied in some detail in previous work by Pietig *et al.*,[32] using the DMFT approximation. These authors found a charge-ordered phase that forms at large values of the intersite interaction, by using a combination of noncrossing approximation, exact diagonalization (ED), and numerical renormalization group calculations. This work demonstrated the increased importance of correlation effects in the CDW phase, leading to the formation of a strongly renormalized quasiparticle with the density of states displaying a narrow peak at the Fermi level. However, the complete V-U phase diagram for this model has not been determined and, more importantly, no evidence for the formation of a Wigner-Mott insulating state has been reported. These and some other interesting aspects of the 2DEG have been clarified in a more recent short paper,[15] where the DMFT equations for the EHM have been solved at low but finite temperature using the recently developed continuous-time quantum Monte Carlo algorithm (CTQMC).[33,34] This work identified the existence of a strongly correlated metallic CDW phase, separating the homogeneous metal from a Wigner-Mott insulating phase present for larger values of the nonlocal interaction and small enough values of the short-range interaction. In contrast, a direct transition between the Fermi-liquid metal and the Wigner-Mott insulating state was found at larger values of the local correlation, triggered by the tendency to charge ordering.

Despite this progress, however, several important physical issues remain to be clarified, in order to correctly understand

the phenomenology of the Wigner-Mott scenario and its possible relevance for the 2DEG problem. In particular, even within the considered DMFT solution of the EHM, the following questions need to be addressed: (1) What are the conditions required to find an intermediate strongly correlated CDW-metallic (CDW-M) phase? (2) What is the temperature dependence of this phase? (3) What is the nature of the phase transitions between the different phases and how does the critical behavior depend on temperature? (4) Is there a regime of phase coexistence between the metal and the insulating state, allowing the possibility of phase separation?

This paper presents careful calculations providing precise and convincing answers to all these questions. In particular, we show the existence of an intermediate CDW-M phase, that separate the homogeneous metal from the Wigner-Mott insulator, for all temperatures smaller than a critical value $T=T_c$. The shrinking of the CDW-M phase corresponds to temperature-dependent behavior of the Wigner-Mott transition, similar to the Pomeranchuk effect.[35] We identify two transitions in the phase diagram of the model, namely, a charge-ordering transition from the homogeneous metal to CDW-metallic state at $V=V_{c1}(T)$ and a Wigner-Mott MIT taking place at $V=V_{c2}(T)$. We demonstrate the continuous character of the MIT for $T<T_c$ and we give clear indications for the existence of phase coexistence, i.e., a sharp first-order transition, at higher temperatures. Furthermore, we present a detailed study of the evolution of the two critical lines V_{c1} and V_{c2} as a function of increasing temperature from $T=0$.

The rest of the paper is organized as follows. In Sec. II, we introduce the main model and the relative notation, together with a brief overview of the (numerical) methods used in this work. In Sec. III, we present the results concerning the Wigner-Mott transition in the EHM and we discuss the related phase diagram. We conclude in Sec. IV, where we present our perspective on the relevance of our picture for the 2DEG and discuss its relation to alternative theoretical scenarios.

II. MODEL AND METHODS

A. Extended Hubbard model

The extended Hubbard model is the simplest model that captures the interplay between strong correlation and charge-ordering effects. This model includes both a local Coulomb interaction, represented by the familiar Hubbard U term, and a nonlocal (intersite) repulsion V. While the presence of this intersite repulsion V may induce the formation of a charge-ordered phase, it also proves capable to enhance the effectiveness of the on-site repulsion U, leading to the formation of a strongly correlated physics even away from integer filling.

The lattice structure of the model is introduced in order to capture the crystalline order of the 2DEG in the low-density regime. The lattice constant is then constrained by the requirement that each cell contains two lattice sites, which can be regarded as precursors of the interstitials and vacancies in the Wigner crystal phase, corresponds to an area of $\pi r_s^2 a_B^2$. The corresponding extended Hubbard model Hamiltonian takes the form

$$H = -t\sum_{\langle ij\rangle\sigma} c_{i\sigma}^{\dagger}c_{j\sigma} + U\sum_{i} n_{i\uparrow}n_{i\downarrow} + V\sum_{ij} n_i n_j - \mu\sum_{i\sigma} n_{i\sigma}. \quad (1)$$

Here, U and V are the on-site and the nearest-neighbor interactions, respectively. The parameter t is the hopping amplitude, $c_{i\sigma}^{\dagger}$ ($c_{i\sigma}$) are the creation (annihilation) operators and $n_i=n_{i\uparrow}+n_{i\downarrow}$ is the occupation number operator on-site i. The chemical potential μ is adjusted to enforce the quarter-filling constraint, corresponding to the presence of one electron per unit cell in the Wigner crystal. Thus, we may expect the formation of a commensurate charge ordering as effect of the intersite repulsion. To this end, we can restrict ourselves to consider a bipartite lattice structure with sublattices A and B.

We solve the problem posed by Hamiltonian (1) using single-site DMFT method,[31] which amounts to mapping the previous lattice problem onto that of a single impurity, coupled to an effective bath, to be self-consistently determined. This approximation becomes exact in the infinite coordination number limit,[36,37] provided the hopping parameter and the intersite interaction are rescaled as $t\to t/\sqrt{z}$ and $V\to 2V/z$. In this limit, the interaction between electrons on neighboring sites i and j are treated in the Hartree approximation, and Hamiltonian (1) assumes the form

$$H = -t\sum_{\langle ij\rangle,\sigma} (c_{ij,\sigma}c_{ij,\sigma}^{\dagger} + \text{H.c.}) - \mu\sum_{i} n_i + U\sum_{i} n_{i\uparrow}n_{i\downarrow} + V\sum_{i\in A, j\in B} (\langle n_i\rangle n_j + n_i\langle n_j\rangle - \langle n_i\rangle\langle n_j\rangle). \quad (2)$$

For simplicity, the terms linear in the occupation operators can be easily absorbed in a redefinition of the chemical potential $\mu_A=\mu-2V\langle n_B\rangle$, $\mu_B=\mu-2V\langle n_A\rangle$. The Weiss field, describing the properties of the effective bath in the DMFT approximation, reads

$$G_{0;A,B}^{-1}(i\omega_n) = i\omega_n - \mu_{A,B} - \Delta_{A,B}(i\omega_n),$$

where $\Delta_{A,B}(i\omega_n)$ is the hybridization function of the associated effective single-impurity Anderson model. The self-consistency condition for the model at hand assumes the following expression:[31]

$$G_{A,B} = \zeta_{B,A}\int_{\mathbb{R}} d\varepsilon \frac{\rho_0(\varepsilon)}{\zeta_A\zeta_B - \varepsilon^2}$$

with $\zeta_{A,B}=i\omega_n+\mu_{A,B}-\Sigma_{A,B}(i\omega_n)$, $\Sigma_{A,B}$ being the *local* self-energy function and $\rho_0(\varepsilon)=\Sigma_{\mathbf{k}}\delta[\varepsilon-\varepsilon(\mathbf{k})]$ the noninteracting density of states corresponding to the chosen lattice. In the following we focus on the simple semicircular model density of states, for which $\rho_0(\varepsilon)=\sqrt{D^2-\varepsilon^2}/4\pi t^2$ with $D=2t=1$ fixing the energy units of the problem. The self-consistency equations then reduce to

$$\Delta_{A,B} = t^2 G_{B,A}. \quad (3)$$

B. Methods

In this section, we briefly review the methods of solutions used in this work, emphasizing the advantages and the drawbacks for each of them. More detailed review of the same methods can be found elsewhere in the literature, cf. Refs.

31, 33, and 38. We begin our discussion with the simplest used impurity solver, namely, the four slave-boson (SB4) method of Kotliar and Ruckenstein.[39] At the mean-field level (saddle point), this method at $T=0$ proves to be equivalent to the well-known Gutzwiller variational approximation but it also allows for extensions to $T>0$. Within the SB4 method, the effective impurity problem is reduced to the solution of a set of algebraic equations for the appropriate slave-boson variational parameters. Solving these equations is a relatively simple task, which allows for quite an accurate numerical solution, and a very precise characterization of the leading critical behavior. Although the SB4 method variationally calculates the Fermi-liquid parameters specifying the quasiparticles and by neglecting incoherent parts of the spectrum, this method is known to generally provide qualitatively and largely even quantitatively accurate solutions when applied within the framework of DMFT theories. In the SB4 approach, the low energy part of the local Green's function is parametrized in terms of the quasiparticle weight Z_i at site i. In the CDW phase these quantities differ on the two sublattices $i=A,B$. The quasiparticle weight $Z_i[e_i,d_i]$ is expressed through the mean-field slave-boson parameters e_i^2 and d_i^2, which are equal to the probability that the site is empty and doubly occupied, respectively. These parameters and ultimately the impurity Green's functions $G_{fA,fB}$, for either the A and the B sublattices, are determined by constrained minimization of a suitable local free energy $\mathcal{F}_i$ parametrized by a Lagrange's multiplier λ_i,

$$\mathcal{F}_i = -\frac{2}{\beta}\sum_{\omega_n} \ln[-i\omega_n - \mu_i + Z_i\Delta_i(i\omega_n)] + Ud_i^2 - \lambda_i(1 - e_i^2 + d_i^2) \tag{4}$$

with $\tilde{\mu}_{A,B}=\mu-2Vn_{B,A}-\lambda_{A,B}$. The (low-energy part of the) ocal Green's functions are determined by the relation $G_{A,B}=Z_{A,B}G_{fA,fB}$. The DMFT equations are closed by supplementing these relation with the self-consistency condition (3). The chemical potential μ and occupation numbers n_A and n_B also have to be calculated self-consistently in order to enforce quarter-filling constraint $n_A+n_B=1$, where $n_{A,B}=\frac{2}{\beta}\Sigma_{\omega_n}G_{fA,B}(i\omega_n)$.

To supplement the SB4 results with more accurate methods we solved the DMFT equation for the EHM with (numerically) exact methods. In particular, in the $T=0$ limit we implemented a density matrix renormalization group (DMRG) impurity solver. The DMRG idea have first been introduced in 1992 by White[40] to deal with one-dimensional quantum lattice problems,[41] for which the Wilson's real-space blocking scheme was observed to fail in describing the correct solution. In more recent work,[38,42] DMRG has been adapted to solve the self-consistent DMFT equations. The algorithm is based on a recursive ED of the associated quantum impurity problem with an increasing size of the effective bath. Similarly to other renormalization-group-based method, the DMRG provides a suitable method to restrict the solution of the effective problem to its relevant subspace. This is achieved using a clever method for limiting the exponential growth of the Hilbert space dimension, based on the analysis of the reduced density matrix. Starting with a small effective bath in the form of two linear chains,[31] the effective impurity problem is exactly solved, and then the size of the bath is recursively increased. At each step the Hilbert space of the problem is constructed using the basis formed by the first M (i.e., the "most probable") eigenvectors of the reduced density matrix $\hat{\rho}=\mathrm{Tr}_{|_{Env}}|gs\rangle\langle gs|$, where $|gs\rangle$ is the (approximated) ground state and the environment is represented by the impurity plus one of the two bath' chains. For every fixed size of the impurity problem, the impurity Green's function are evaluated using successive applications of the Lanczos' method.[43] The self-consistency condition (3) is then used to update the Hamiltonian parameters of the problem.

The recursive nature of the DMRG method permits a systematic improvement of the quality of the solution. In addition, this method has the advantage of treating on the same footing both low- and high-energy scales, in contrast to standard RG technique, which principally focus on the low-energy spectra of the problem. However, the particular one-dimensional topology imposed by the DMRG algorithm makes this method suffering of the finite-size effects. In practice effective baths as large as $L=20$ sites have to be reached in order to obtain a satisfying solution of the model.

While the DMRG algorithm it is straightforward at zero temperature, its extensions to finite-temperature regime are nontrivial. To this end, we have solved the DMFT equations using alternative algorithms. The first finite-temperature method is (complete) exact diagonalization of the discretized effective impurity problem. This method permits to access the full spectrum of the problem, thus allowing for the calculation of the exact impurity Green's function and other observables. The Hamiltonian parameters are self-consistently determined using an adaptive method that permits to minimize the (in principle, large) finite-size effects.[44] This method is indeed known to have an almost constant scaling with the bath' size. On the other hand, a small number of degrees of freedom in the problem prevents the access to the very low-energy physics of the model, thus a significant number of bath' sites ($N_s>5$) becomes necessary to have a good description of the model solution. Our calculation has been performed using $N_s=7$, which is the largest accessible number of sites for this method.

The second method we used to solve the DMFT equations at finite temperature is the continuous-time quantum Monte Carlo, in the implementation of Ref. 33. The CTQMC is a statistically exact method based on the Monte Carlo samplings of the diagrams obtained by perturbative expansion of the impurity problem with respect to the hybridization. The CTQMC algorithm of Ref. 33 has proven to be a highly reliable and stable method, that permits to capture the low-temperature regime of the model. On the other hand, the statistical nature of the method put some, indeed nonstringent, limitations to its applicability in the proximity of a phase transition. In this regime, the solution requires a very large number of Monte Carlo samplings and a large number of iterations of the self-consistency algorithm to overcome the enhanced fluctuations and the critical slowing down of the solution.

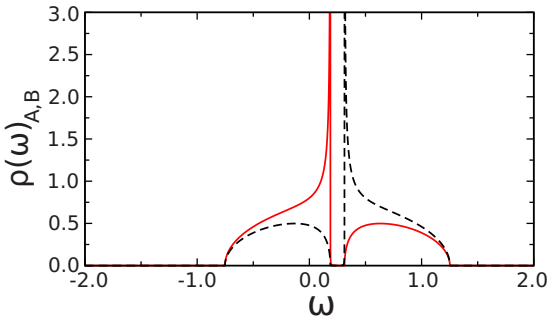

FIG. 1. (Color online) Noninteracting DOS of sublattice A (solid line) and B (dashed line) for $\delta \simeq 0.2$. The system is in a CDW-M state and correspondingly the DOS is split in two lobes. The Fermi energy, corresponding to $\omega=0$, falls inside the lower lobe as results of the quarter-filling constraint.

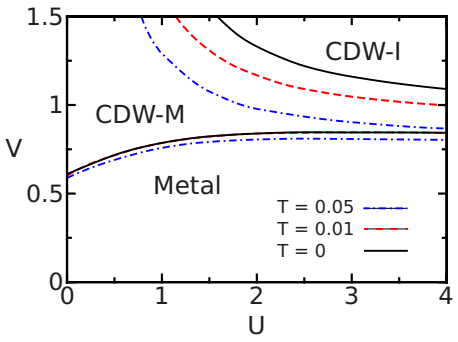

FIG. 2. (Color online) DMFT phase diagram of the extended Hubbard model obtained with a slave-boson (SB4) impurity solver. The figure shows the phase boundaries obtained for different values of the temperature T. At $T=0$ (solid line), the solution shows the existence of a large CDW-metallic phase at all values of the local correlation U. This region narrows as the temperature T is increased from zero to $T=0.01$ (dashed line) to $T=0.05$ (dotted-dashed line) but it never disappears.

C. $U=0$ solution

In the noninteracting limit $U=0$, the problem posed by Hamiltonian (2) can be easily solved analytically. In particular, here we are interested in obtaining the analytic solution corresponding to the DMFT approximation, in order to get some physical insight from the model. In the noninteracting limit the DMFT equations can be recast in the form

$$G_A^{-1}(z) = z + \mu_A - t^2 G_B = \alpha - t^2 G_B,$$

$$G_B^{-1}(z) = z + \mu_B - t^2 G_A = \beta - t^2 G_A \tag{5}$$

and solved for, say, G_A giving

$$G_A = 2[\beta \pm \sqrt{\beta^2 - \beta/\alpha}].$$

All the solutions to this equation can be expressed in terms of a single parameter $\delta=n_A-n_B$ representing the occupation imbalance between the two sublattices. The density of states is nonzero only in the energy interval defined by the $\beta^2 - \beta/\alpha < 0$ condition. The system undergoes a charge ordering at $V=V_c$ with the formation of a spectral gap $\Delta=V\delta$ (for $V \geq V_c$). In this regime, the original quarter-filled band splits into two bands, but the Fermi level remains inside the lowest band, which remains half-filled, cf. Fig. 1. Thus a spectral gap at the Fermi level can only be opened by increasing the local correlation U.

In this limit, we can think at the system as consisting of one sublattice A with occupation close to half filling, and the other B as being nearly empty. An estimate of the effective hopping between sites in the sublattice A can be obtained integrating out (virtual) high-energy processes, corresponding to hops through the sites of sublattice B. At $V \gg t$, to leading order the effective hopping between the sites of the A sublattice then takes the form $t_{eff}=t^2/V$.

III. WIGNER-MOTT TRANSITION

A. Phase diagram

In this section, we present results concerning the phase diagram of the EHM as a function of the local correlation U and the intersite interaction V. In the following we use different methods to investigate the various phases of the system as a function of the temperature T.

Our results show the existence of three qualitatively different phases, which can be classified by two order parameters: (i) the CDW staggered density $\delta=n_A-n_B$ and (ii) the quasiparticle residue (i.e., renormalization constant) $Z_{A,B}$ at each sublattice. The different phases of the model are characterized as following: (a) *Fermi liquid.* A featureless homogeneous metallic state, corresponding to $n_A=n_B=1/2$ and $Z_A=Z_B>0$. (b) *CDW-M.* A CDW-ordered metallic state with $n_A>n_B$ and $Z_B>Z_A$. The sublattice A has an occupation near to the half-filling condition ($n_A \simeq 1$), thus closer to Mott localization. As a consequence of this the quasiparticles weight Z_A is substantially reduced, corresponding to a enhancement of their effect mass $m_A^*/m_A \simeq Z_A^{-1}$. (c) *CDW-I.* A Wigner-Mott insulating phase. In this regime $n_A \gg n_B$ but while $Z_B \sim 1$, sublattice A has an identically zero quasiparticle weight $Z_A=0$. This corresponds to the Mott localization of the electrons on the "nearly half-filled" sublattice A.

The U-V phase diagram as obtained from our SB4 solution for increasing values of the temperature T is presented in Fig. 2. At zero temperature, we obtain a continuous transition from the homogeneous metallic phase to the CDW metal. This is followed by a second continuous transition to the CDW insulator as the intersite interaction V is further increased. The intermediate CDW metallic phase, while decreasing in size at large U, remains of finite extent even in the limit $U \to \infty$ limit. Upon increasing the temperature T, we observe a shrinking of the intermediate CDW-M phase at large values of U. Still, no signs for the disappearance of this phase have been observed with the slave-bosons methods. This result is in contrast to that initially obtained in Ref. 15 at very low but finite temperature $T=0.01$ using a more sophisticated method. Despite the qualitative validity of the SB4 method, this result clearly puts in question the main features of the phase diagram for the EHM. In particular, it suggests that the intermediate CDW-M phase at intermediate to large U is very fragile to temperature. This observation calls for a more detailed study of the temperature depen-

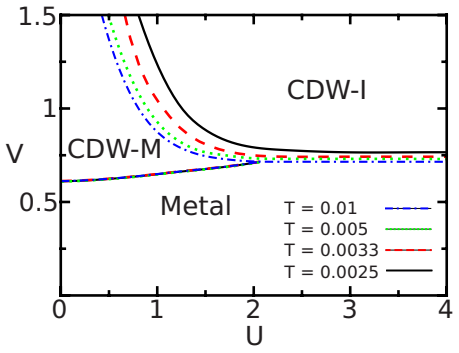

FIG. 3. (Color online) DMFT phase diagram of the extended Hubbard model obtained with CTQMC method. The results illustrate the evolution of the phase boundaries for the Mott-Wigner transition as a function of increasing temperature. For the lowest value of the temperature $T=0.0025$ (solid line), we observe the well established presence of a CDW-M separating the homogeneous metal from the CDW insulator. This phase region narrows upon increasing the value of the temperature to $T=0.0033$ (dashed line) and $T=0.005$ (dotted line), till a closure of the phase boundaries is observed for $T\sim 0.01$ (dotted-dashed line) at $U\sim 2$.

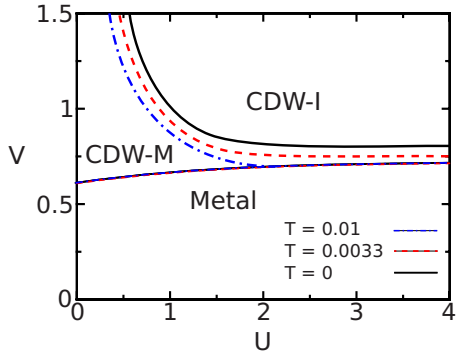

FIG. 4. (Color online) DMFT phase diagram of the extended Hubbard model obtained with DMRG (zero temperature) and ED (finite temperature) impurity solvers. The figure shows the evolution of the phase boundaries as a function of increasing temperature from $T=0$ (solid line) to $T=0.0033$ (dashed line), to $T=0.01$ (dotted-dashed line). The intermediate CDW-M observed at $T=0$ is found to narrows upon increasing the temperature, until a closure of the boundary lines is obtained around $U\sim 2$ and for $T\sim 0.01$. The DMRG results have been obtained with a bath of $L=30$ sites whereas the ED calculation have been performed with a number of sites $N=7$.

dence of the metal-insulator phase boundary, which we examine in the following sections.

The results from CTQMC solution of the DMFT equations for the EHM are summarized in the phase diagram in Fig. 3. While this method cannot capture the zero-temperature properties of the model, it provides an excellent and reliable solution at very-low temperature scales. At the lowest accessible temperature $T=0.0025$, we observe a continuous transition between a homogeneous metallic state to a CDW metal for low values of V and every value of U. At this value of the temperature, the CDW-M phase is found to be destabilized toward a CDW-insulating phase upon increasing the intersite interaction V. Upon increasing the temperature, we observed a narrowing of the intermediate CDW-M in favor of the Wigner-Mott insulating state, until a merge of the boundary lines is observed for temperatures of the order $T\sim 0.01$ (that is two orders of magnitude smaller than the bare bandwidth).

To better clarify the issue of closing boundary lines at low temperature, we have solved the DMFT equations with an exact method at zero temperature, i.e., the DMRG. Furthermore, we have complemented this investigation with a powerful ED solver, in order to access the finite-temperature properties of the system. The ED-DMRG results for the extended Hubbard model problem are condensed in the U-V phase diagram presented in Fig. 4. The phase diagram is in very good agreement with that obtained from the CTQMC solution of the model, already presented in Fig. 3. Our calculations confirm the existence of an homogeneous metallic phase at low values of V and any value of the local correlation U. The stability of the homogeneous metallic phase is related to the quarter-filling condition, making the local interaction nearly ineffective at small V. For any fixed value of U and for V larger than a critical value V_{c1} almost independent of the temperature T, the system shows a continuous phase transition toward a CDW-M state. The evolution of the two sublattices upon further increasing V is different. One sublattice gets nearly empty and becomes, for sufficiently large U, a band insulator. The other sublattice, with a filling closer to 1, undergoes a continuous Mott transition toward a CDW-insulating state for U large enough and V larger than a critical value V_{c2} weakly depending on the temperature T. In particular the zero-temperature solution of the model shows the persistence of the intermediate CDW-M for any value of the local correlation U. This phase is observed to narrow upon increasing the temperature until a closure of the boundary lines at $U\sim 2$ is obtained for $T\sim 0.01$, in excellent agreement with the CTQMC solution of the model.

B. Generalized Pomeranchuk effect

Next, we would like to discuss the physical implications of the observed temperature evolution of the phase diagram, in relation to the interesting nonmonotonic resistivity behavior observed in very clean 2DEG samples.[5] As a general trend, we observed a shrinking of the CDW-M region as temperature is increased from $T=0$. This effect is most pronounced at the CDW-M to CDW-I boundary $V_{c2}(U)$, i.e., in the region where a heavy Fermi-liquid forms. From the physical point of view, this temperature-dependent behavior reflects the entropy gained in destroying the (heavy) Fermi liquid to form localized magnetic moments in the Wigner-Mott (CDW-I) phase. This mechanism of entropy release is indeed similar to that anticipated in the early work of Pomeranchuk,[45] who speculated about the general problem finite-temperature solidification of ^{3}He.[35]

It should be emphasized, however, that this "entropic" destruction of a strongly correlated Fermi liquid is a very general phenomenon, which does not necessarily require a first-order phase transition, as postulated by Pomeranchuk, or a phase coexistence with separation of the phases.[46–49] For example, the same effect can be observed in many heavy-

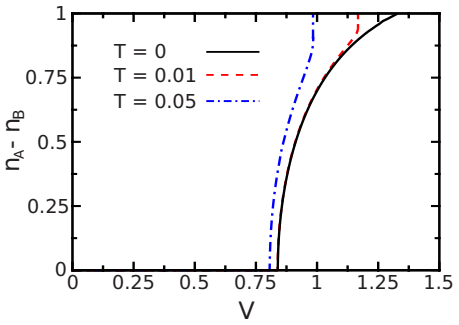

FIG. 5. (Color online) Order parameter $\delta = n_A - n_B$ as a function of the intersite interaction V, for $U=2$ and increasing values of the temperature T. The metallic CDW phase appears for $V > V_{c1} \simeq 0.84$ while a CDW insulator forms for $V > V_{c2} \simeq 1.35$. Within DMFT-SB4 solution, the $T=0$ transition is continuous while for $T > 0$ a small discontinuity in CDW order parameter is observed, that is a possible artifact of the method.

fermion systems, where the destruction of the heavy Fermi liquid for temperatures larger than the "coherence" temperature $T^* \sim T_K$, coincides with a release of extensive spin entropy $S \sim k_B \ln 2$, corresponding to the localization of the f electrons. The corresponding resistivity maximum represents a temperature-driven crossover rather than a sharp phase transition, related to the fact that the two phases do not have to differ by symmetry. In the Wigner-Mott picture of the 2DEG, we thus recognize in the entropy of the high-temperature state as the driving force for electron localization.

C. Charge ordering

To better understand the nature of the continuous transitions observed in the phase diagrams of Sec. II, we now investigate the behavior of the charge-order parameters $\delta = n_A - n_B$ as a function of V for different values of the temperature. The symmetry breaking associated to this transition corresponds to the occupation unbalance in favor of one of the two sublattices and the order parameter δ roughly measures the tendency of the system to form charge-ordered phase. All the following results have been obtained for a fixed value of the local correlation $U=2$, corresponding to a region of the phase diagram with narrowing intermediate CDW-M phase separating the Wigner-Mott insulator from the homogeneous metal.

Results from SB4 method are presented in Fig. 5. The figure shows, at $V=V_{c1}$, the emergence of a charge-ordering instability which emerges before the Fermi-liquid state is destroyed. At $T=0$ the slave-bosons solution displays the conventional critical square-root behavior for the order parameter, i.e., $\delta = (V - V_{c1})^{1/2}$. At finite temperature, however, a small "jump" in the order parameter can be observed, that is believed to be an artifact of the SB4 method. In the following, we shall clarify the character of the transition using numerically exact methods, namely, the CTQMC and DMRG at finite and zero temperature, respectively.

The DMRG results for the charge ordering at zero temperature are shown in Fig. 6(a). We observe a sharp increasing of the order parameter for $V \sim V_{c1}$ with a typical square-rootlike critical behavior for higher values of the intersite correlation. This result is in good agreement with that obtained with SB4 method at $T=0$, although the finite size of the DMRG effective problem does not permit to exactly locate the critical value of V. On the other hand, no trace of any discontinuities for the order parameter has been observed at finite temperature, using CTQMC [cf. Fig. 6(b)] and finite-temperature exact diagonalization method (not shown). Thus, our results put strong evidences for the continuous character of the charge-ordering transition, irrespective of the value of the temperature.

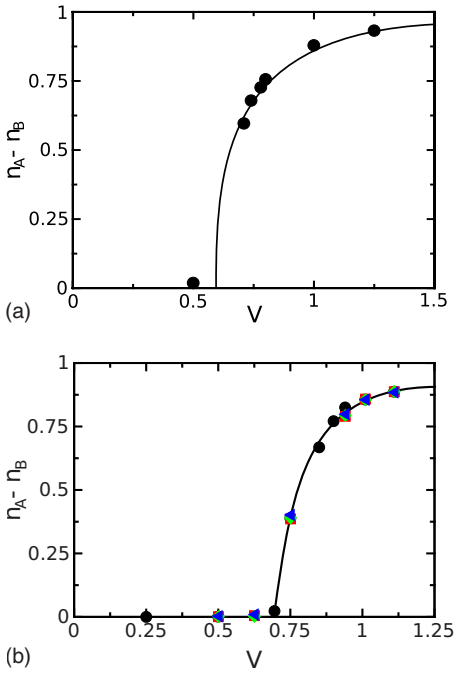

FIG. 6. (Color online) The two panels show the behavior of the order parameter $\delta = n_A - n_B$ as a function of intersite interaction V, for $U=2$ and different values of the temperature T. (a) Results from zero-temperature calculation performed using the DMRG solver. (b) DMFT-CTQMC solution for several temperatures $T=0.01$ (dots), 0.005 (squares), 0.0033 (diamond), 0.0025 (triangles). Both $T=0$ and finite-temperature calculations display a rather conventional $(V - V_{c1})^{1/2}$ critical behavior near the CDW transition, similar to that observed in the noninteracting limit.

D. Critical behavior

Finally we have investigated the destruction of the charge-ordered metallic state in favor of the Wigner-Mott insulator, driven by the increasing intersite correlation V and for large values of the local interaction U. As V increases, the effective hopping amplitude at the nonempty sublattice $t_{eff} = t^2/V$ decreases. Thus, it is reasonable to expect that for $U \sim t_{eff}$ a Wigner-Mott transition takes place. Our results, obtained with different methods, substantiate this qualitative picture. We observe in fact a Wigner-Mott transition for $V_{c2}(U) \sim t_{eff}^2/U$, that is compatible with the observed $1/U$ behavior for the CDW metal to insulator transition line in the phase diagram (cf. Sec. II). In the following, we present a

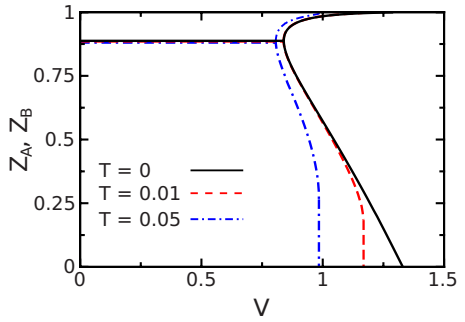

FIG. 7. (Color online) Quasiparticle weight $Z_{A,B}$ as a function of V for different temperatures and $U=2$. At $T=0$ (solid line), we observe a linear vanishing of the nonempty sublattice renormalization constant while the constant corresponding to nearly empty sublattice flows to one. At larger value of the temperature $T=0.01$ (dotted-dashed line) and $T=0.05$ (dashed line) the DMFT-SB4 predicts a small jump in the quasiparticle weight, that is a possible artifact of the method rather than a real discontinuity of the transition.

characterization of the Wigner-Mott transition in the EHM in terms of the vanishing of the renormalization constants $Z_{A,B}$.

Results obtained with SB4 method are presented in Fig. 7. At $T=0$, the quasiparticle weight for the nearly half-filled sublattice, say A, is found to have a linearly vanishing behavior $Z_A \simeq (V_{c2}-V)$, similar to that observed in the conventional Mott scenario. At finite temperature, the SB4 shows again the breakdown of the solution, leading to unphysical jump in the renormalization constant behavior. This issue has been clarified using the more sophisticated CTQMC method

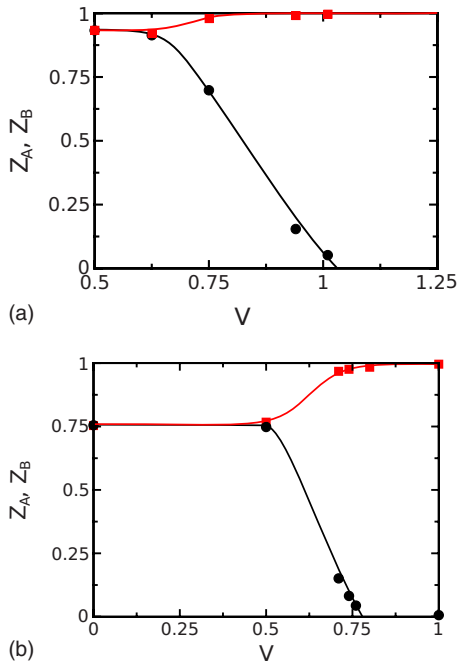

FIG. 8. (Color online) Quasiparticle residues $Z_{A,B}$ behavior as a function of V and $U=2$ at (a) $T=0.01$ and (b) zero temperature. The figures show the linear vanishing of the order parameter of the Wigner-Mott transition, independent of the value of the temperature and expressing the continuous character of the transition.

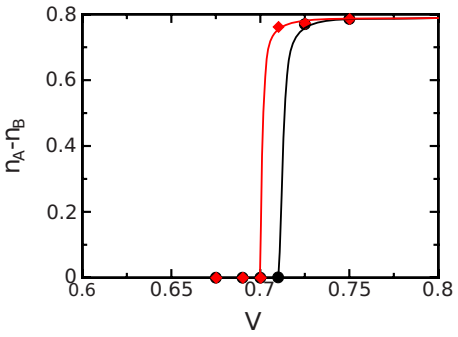

FIG. 9. (Color online) Order parameter $\delta=n_A-n_B$ as a function of the nonlocal interaction V. Data are obtain from CTQMC calculations at $T=0.01$ and $U=3$. The figure illustrates the first-order character of the direct transition between the homogeneous metal and the Wigner-Mott insulator, presenting evidences for the coexistence of the metallic and insulating phases in a narrow interval around V_{c2}.

at finite temperature. Results from CTQMC calculations at low temperature are shown in Fig. 8(a). The renormalization constant for the nonempty sublattice is found to have a linear vanishing behavior as observed within the SB4 solution at $T=0$, thus indicating the continuous character of the Wigner-Mott transition. A very similar behavior is observed in the zero-temperature model calculations performed with DMRG and presented in Fig. 8(b).

The continuous transition from the correlated CDW-metallic phase with $m^*>1$ to the Mott-Wigner insulator, observed at temperatures $T<T_c \simeq 0.01$ and local interaction large enough $U>2$, is replaced at higher temperature $T>T_c$ by a sharp first-order transition from the homogeneous metal with $m^* \simeq 1$ directly to the CDW-insulating state. This is compatible with the shrinking and disappearance of the intermediate correlated CDW-metallic state with increasing temperature. This effect is well illustrated in Fig. 9, presenting the tiny hysteresis cycle of the order parameter $\delta=n_A-n_B$ for a large value of the correlation $U=3$ and $T=0.01$. The two curves in the figures are obtained following the metallic and the insulating solutions, respectively. As we can clearly see, the two solutions have a small region of coexistence around the transition point at $V=V_{c2}$, indicating the first-order character of the Wigner-Mott transition at $T>T_c$.

Interestingly, no trace of first-order transition has been found in the less correlated regime $U<2$, which is more relevant for the interpretation of the experimental results. In this regime, the correlated quasiparticles are gradually destroyed by the thermal fluctuations at $T>T^* \sim Z$, leading to a thermal metal to insulator crossover with an associated resistivity maximum, but without phase separation or any first-order transition,[47] compatible with out interpretation in terms of generalized Pomeranchuk effect.

IV. CONCLUSIONS AND PERSPECTIVES

In this work we investigated the quarter-filled extended Hubbard model, in order to describe the essential features of the Wigner-Mott metal-insulator transitions. Using single-

site DMFT theory, we obtained the U-V phase diagram, and carefully studied its evolution as a function of temperature. For this model, a metallic charge-ordered phase (CDW-M) is generally found at low temperatures, separating a Wigner-Mott insulator at strong coupling from a homogeneous Fermi liquid at weak coupling. This intermediate CDW-M phase is the one showing the most interesting features, chiefly the emergence of strong correlation effects signaled by large effective mass m^* enhancements. Physically, this reflects the presence of heavy quasiparticles existing only below a characteristic energy scale $E^* \sim T_F/m^*$, which vanishes at the metal-insulator transition. Indeed, we predict that such a correlated metallic state can easily be suppressed either by increasing the temperature beyond a modest temperature $T^* \sim E^*$, or by applying modest polarization fields $H^* \sim T^*$—in striking agreement with the experiments.[5] In addition, we demonstrated that the region occupied by the CDW-M phase shrinks as a function of increasing temperature, thus producing an interesting Pomeranchuk-type effect. We presented an interpretation of this effect in terms of the entropic destruction of the strongly renormalized Fermi liquid (CDW-M) in favor the Wigner-Mott insulator, similar to the early idea proposed by Pomeranchuk in the context of the ^{3}He solidification.

The extended Hubbard model we used certainly cannot be regarded as a realistic or quantitatively accurate representation of the 2DEG materials. Ours is an approach complementary to that provided by first-principles (e.g., diffusion Monte Carlo) studies of realistic models[50] of 2DEG—yet with surprisingly similar results. Both approaches portray a picture of a strongly correlated electron fluid featuring a single characteristic energy scale. But precisely by virtue of its simplicity, our model calculation makes it possible to unravel *the mechanism* behind the puzzling behavior in the metal-insulator transition region. It demonstrates how the tendency to charge ordering reinforces the transmutation of conduction electrons into local magnetic moments—a fundamental physical process behind the phenomenon Wigner-Mott localization.

Many quantitative aspects of our model can and should be improved. In particular, our lattice model does not do justice to dynamical charge fluctuations, which should further enhance the role of Coulomb correlations even in absence of long-range charge order. Indeed, results supporting the robustness of the intermediate correlated metallic phase, have been recently obtained in Ref. 51 using complementary methods which emphasized the important role of longer-range Coulomb interactions. In addition, the influence of disorder also needs to be addressed in the context of the Wigner-Mott scenario we propose. These effects can be naturally incorporated in our framework using the recently developed "extended" DMFT approaches.[52,53] This interesting and important task opens an interesting avenue for future work.

ACKNOWLEDGMENTS

The authors thank S. Fratini and J. Merino for useful discussions. D.T. acknowledges the Serbian Ministry of Science and Technological Development under Project No. OI 141035; NATO Science for Peace and Security Programme Reintegration under Grant No. EAP.RIG.983235. V.D. was supported by the NSF under Grant No. DMR-0542026. K.H was supported by the NSF under Grant No. DMR-0746395. G.K. was supported by the NSF under Grant No. DMR-0906943.

[1] E. Abrahams, P. W. Anderson, D. C. Licciardello, and T. V. Ramakrishnan, Phys. Rev. Lett. **42**, 673 (1979).
[2] B. L. Altshuler, A. G. Aronov, and P. A. Lee, Phys. Rev. Lett. **44**, 1288 (1980).
[3] G. J. Dolan and D. D. Osheroff, Phys. Rev. Lett. **43**, 721 (1979).
[4] D. J. Bishop, D. C. Tsui, and R. C. Dynes, Phys. Rev. Lett. **44**, 1153 (1980).
[5] S. V. Kravchenko, G. V. Kravchenko, J. E. Furneaux, V. M. Pudalov, and M. D'Iorio, Phys. Rev. B **50**, 8039 (1994).
[6] D. Popović, A. B. Fowler, and S. Washburn, Phys. Rev. Lett. **79**, 1543 (1997).
[7] Y. Hanein, U. Meirav, D. Shahar, C. C. Li, D. C. Tsui, and H. Shtrikman, Phys. Rev. Lett. **80**, 1288 (1998).
[8] E. Abrahams, S. V. Kravchenko, and M. P. Sarachik, Rev. Mod. Phys. **73**, 251 (2001).
[9] S. V. Kravchenko and M. P. Sarachik, Rep. Prog. Phys. **67**, 1 (2004).
[10] A. A. Shashkin, S. V. Kravchenko, V. T. Dolgopolov, and T. M. Klapwijk, Phys. Rev. B **66**, 073303 (2002).
[11] G. Zala, B. N. Narozhny, and I. L. Aleiner, Phys. Rev. B **64**, 214204 (2001).
[12] T. Okamoto, K. Hosoya, S. Kawaji, and A. Yagi, Phys. Rev. Lett. **82**, 3875 (1999).
[13] A. Punnoose and A. M. Finkel'stein, Phys. Rev. Lett. **88**, 016802 (2001).
[14] S. Pankov and V. Dobrosavljevic, Phys. Rev. B **77**, 085104 (2008).
[15] A. Camjayi, K. Haule, V. Dobrosavljevic, and G. Kotliar, Nat. Phys. **4**, 932 (2008).
[16] E. Wigner, Phys. Rev. **46**, 1002 (1934).
[17] G. Giuliani and G. Vignale, *Quantum Theory of the Electron Liquid* (Cambridge University Press, Cambridge, England, 2005).
[18] A. M. Finkel'stein, Z. Phys. B: Condens. Matter **56**, 189 (1984).
[19] C. Castellani, C. Di Castro, P. A. Lee, and M. Ma, Phys. Rev. B **30**, 527 (1984).
[20] M. Vojta, A. Hübsch, and R. M. Noack, Phys. Rev. B **63**, 045105 (2001).
[21] H. Seo, J. Merino, H. Yoshioka, and M. Ogata, J. Phys. Soc. Jpn. **75**, 051009 (2006).
[22] T. Takahashi, Y. Nogami, and K. Yakushi, J. Phys. Soc. Jpn. **75**, 051008 (2006).
[23] N. P. Ong and R. J. Cava, Science **305**, 52 (2004).
[24] J. Merino, B. J. Powell, and R. H. McKenzie, Phys. Rev. B **79**,

161103 (2009).
[25] R. H. McKenzie, J. Merino, J. B. Marston, and O. P. Sushkov, Phys. Rev. B **64**, 085109 (2001).
[26] O. I. Motrunich and P. A. Lee, Phys. Rev. B **70**, 024514 (2004).
[27] J. Merino, B. J. Powell, and R. H. McKenzie, Phys. Rev. B **73**, 235107 (2006).
[28] J. Wahle, N. Blümer, J. Schlipf, K. Held, and D. Vollhardt, Phys. Rev. B **58**, 12749 (1998).
[29] Y. Ōno, R. Bulla, and A. C. Hewson, Eur. Phys. J. B **19**, 375 (2001).
[30] J. Merino, Phys. Rev. Lett. **99**, 036404 (2007).
[31] A. Georges, G. Kotliar, W. Krauth, and M. J. Rozenberg, Rev. Mod. Phys. **68**, 13 (1996).
[32] R. Pietig, R. Bulla, and S. Blawid, Phys. Rev. Lett. **82**, 4046 (1999).
[33] K. Haule, Phys. Rev. B **75**, 155113 (2007).
[34] P. Werner, A. Comanac, L. de' Medici, M. Troyer, and A. J. Millis, Phys. Rev. Lett. **97**, 076405 (2006).
[35] R. C. Richardson, Rev. Mod. Phys. **69**, 683 (1997).
[36] W. Metzner, Phys. Rev. B **43**, 8549 (1991).
[37] W. Metzner and D. Vollhardt, Phys. Rev. Lett. **62**, 324 (1989).
[38] D. J. García, K. Hallberg, and M. J. Rozenberg, Phys. Rev. Lett. **93**, 246403 (2004).
[39] G. Kotliar and A. E. Ruckenstein, Phys. Rev. Lett. **57**, 1362 (1986).
[40] S. R. White, Phys. Rev. Lett. **69**, 2863 (1992).
[41] U. Schollwöck, Rev. Mod. Phys. **77**, 259 (2005).
[42] D. J. García, E. Miranda, K. Hallberg, and M. J. Rozenberg, Phys. Rev. B **75**, 121102 (2007).
[43] K. A. Hallberg, Phys. Rev. B **52**, R9827 (1995).
[44] M. Caffarel and W. Krauth, Phys. Rev. Lett. **72**, 1545 (1994).
[45] I. Pomeranchuk, Zh. Eksp. Teor. Fiz. **90**, 919 (1950).
[46] R. Jamei, S. Kivelson, and B. Spivak, Phys. Rev. Lett. **94**, 056805 (2005).
[47] B. Spivak and S. A. Kivelson, Phys. Rev. B **70**, 155114 (2004).
[48] B. Spivak, Phys. Rev. B **67**, 125205 (2003).
[49] B. Spivak, Phys. Rev. B **64**, 085317 (2001).
[50] G. Fleury and X. Waintal, Phys. Rev. B **81**, 165117 (2010).
[51] S. Fratini and J. Merino, Phys. Rev. B **80**, 165110 (2009).
[52] S. Pankov and V. Dobrosavljević, Phys. Rev. Lett. **94**, 046402 (2005).
[53] E. Miranda and V. Dobrosavljevic, Rep. Prog. Phys. **68**, 2337 (2005).